

STATISTICAL STUDY OF THE CORRELATION OF
HARD X-RAY AND TYPE III RADIO BURSTS
IN SOLAR FLARES

Russell J. Hamilton ¹ and Vahé Petrosian ²

Center for Space Science and Astrophysics

Stanford University

Stanford, California 94305

CSSA-ASTRO-89-03

NASG-4092

May 1989

Submitted to *The Astrophysical Journal*

National Aeronautics and Space Administration Grant NSG-7092

National Science Foundation Grant ATM 8705084

¹ Also Department of Physics, Stanford University

² Also Department of Applied Physics, Stanford University

Abstract

We have analyzed a large number of hard X-ray events which were recorded by the Hard X-Ray Burst Spectrometer (HXRBS) on the Solar Maximum Mission (SMM) during the maximum of the 21st solar cycle (circa 1980) in order to study their statistical correlation with type III bursts. We confirm qualitatively the earlier finding by Kane (1981) that flares with stronger hard X-ray emission, especially those with harder spectra, are more likely to produce a type III burst. The observed distribution of hard X-ray and type III events and their correlations are shown to be satisfactorily described by a bivariate distribution consistent with the assumption of statistical linear dependence of X-ray and radio burst intensities. From this analysis we determine the distribution of the ratio of X-ray intensity (in counts/s) to type III intensity (in solar flux units) which has a wide range and a typical value for this ratio of about 10. The implications of our results for impulsive phase models are discussed.

Subject headings: Sun: flares – Sun: radio radiation – Sun: x-rays

I. Introduction

It is generally accepted that the electrons which produce the impulsive hard X-ray bursts and those which cause the type III radio emissions during a solar flare have a common origin. The hard X-rays are a result of bremsstrahlung radiation of electrons which penetrate to the lower corona and chromosphere while type III radiation is produced by those electrons which escape on open field lines generating plasma turbulence as they travel away from the sun. The correlation of hard X-ray emission with type III emission has been studied both statistically (Kane 1981) and by detailed analysis of individual events (see e.g. Kane, Pick, and Raoult 1980, Kane, Benz, and Treumann 1982, Dennis *et al.* 1984, or Raoult *et al.* 1985). There is a wide variation in the relative strengths of the hard X-ray and type III bursts. In fact, the majority of hard X-ray events are not accompanied by an identifiable type III burst and vice versa. From this data one can estimate the ratio of the number of electrons involved in the production of hard X-rays to those producing type III radiation. For example, Ramaty *et al.* (1980) estimates an average value of 10^2 to 10^4 for this ratio. However, the range of this ratio is very large. In some hard X-ray events with no detectable type III burst this number must exceed 10^7 (Simnett and Benz 1986).

This kind of information is not very useful in the theoretical understanding of the phenomena. A knowledge of the mean value and dispersion (or in general the distribution) of such a ratio would be much more useful. To obtain such information from data with large dispersion a statistical approach to study the relationship between these two emission mechanisms is essential. A statistical study can establish the general trends in the data (such as mean values and dispersion) and therefore be helpful in the understanding of the general behavior of flares, such as the directionality of the accelerated electrons and the magnetic field configuration surrounding the acceleration region. Kane's (1981) investigation dealt with the correlation of the X-ray and type III emissions observed during the solar maximum of the 20th solar cycle (circa 1969). He found that the correlation between X-ray and type III events increased with the intensity and starting frequency of

the type III burst, and with the peak energy flux and spectral hardness of the hard X-ray burst. He concluded that the observations suggest that the acceleration region is located in the corona and that the electrons responsible for both emissions are accelerated in a single process. The observed correlations were shown to be consistent with a bivariate distribution function of X-ray and type III burst intensities by Petrosian and Leach (1983, hereafter PL). Although the distribution could not be determined from Kane's data, a procedure was outlined for the determination of the distribution given a larger data set with better resolution of radio burst intensities. Therefore, we decided to look at a large sample of flares which had either a hard X-ray event or a type III burst for the most recent solar maximum and to apply the method of PL to determine the bivariate distribution function and discuss the resulting implications.

The paper is organized as follows. In the next section, we describe the data set that we analyzed. In §III, we use the data to find the resulting bivariate distribution function and discuss its properties. A discussion of our results is given in §IV and a brief summary in §V.

II. Data

The hard X-ray events were obtained from the tables in the Hard X-Ray Burst Spectrometer Event Listing 1980 to 1987 (Dennis *et al.* 1988) excluding events which were interrupted or were nonsolar in origin. The radio data consisted of observations made at Bleien (BLEN) and at the Osservatorio Astronomico Di Trieste (Trieste) tabulated in their quarterly report *Osservazioni Solari*. These data were accumulated and kindly made available to us by Dr. A.O. Benz. The BLEN data does not give a precise quantitative measure of the strength of the type III bursts such as the flux density. Consequently, we use the Trieste data which gives the peak fluxes, the start time, the peak time, and the duration of the burst at 237, 327, and 408 MHz for our analysis.

For our study, a hard X-ray event and a type III burst are considered to be associated

if the peak in the radio flux occurred during the duration of the hard X-ray burst or the peak in the count rate of the HXRBS detector occurred during the duration of the radio burst. We studied bursts which occurred during the maximum of the 21st solar cycle from the beginning of the HXRBS data record 1980 February 19 until 1981 September 30. During this period 3490 HXRBS events were recorded which are included in our study and we have X-ray spectral information for 241 of these bursts which was kindly made available to us by Dr. B.R. Dennis. There were 944 recorded bursts at 237 MHz during this same period of time with 134 of these bursts correlated with a hard X-ray burst. Table 1 summarizes the statistics of the hard X-ray and the 237 MHz radio data used in our analysis below.

III. Analysis of the Correlation

a) Distribution of Burst Intensities

For the purpose of description of the distribution of bursts, we choose the readily available peak count rate of the hard X-ray bursts and peak flux density at 237 MHz (in solar flux units which is equal to $10^{-22} \text{Wm}^{-2} \text{Hz}^{-1}$) for the radio bursts which we denote by X and R, respectively. The choice of the 237 MHz channel is somewhat arbitrary, but similar results are found for all three radio channels.

Figure 1 shows the distribution of the 134 correlated events (those with both X-ray and radio fluxes) in the R-X plane. This figure shows the wide range of the fluxes in both energy bands with no apparent clear correlation between X and R. Instrumental cut-off seems to be at 20 or 30 counts per second for X-rays and about 50 to 100 solar flux units at 237 MHz. We let the number of bursts with intensities in the range X to X+dX and R to R+dR be $Af(X, R)dXdR$, where $f(X, R)$ is the distribution function of the bursts (normalized to unity) and A is the total rate of occurrence of all bursts. The moments of this function are useful for demonstrating the existence of a correlation between the occurrence of a hard X-ray burst of intensity X and the occurrence of a type III burst of

intensity R .

From the bivariate distribution $f(X, R)$, the number of hard X-ray bursts with intensity between X and $X+dX$ with radio intensity greater than R_o is

$$N_{R_o}(X) = A \int_{R_o}^{\infty} f(X, R) dR . \quad (1)$$

Similarly, the number of type III bursts with intensity between R and $R+dR$ with X-ray intensity greater than X_o is

$$N_{X_o}(R) = A \int_{X_o}^{\infty} f(X, R) dX . \quad (2)$$

For $R_o = 0$, equation (1) gives the distribution $N_o(X)$ of peak count rates of all X-ray bursts. Similarly, $N_o(R)$ gives the distribution of radio fluxes of all type III bursts. If the radio and the hard X-ray intensities are stochastically independent of each other then the distribution is separable; $f(X, R) = A\psi(X)\phi(R)$. For this situation equations (1) and (2) become

$$N_{R_o}(X) = A\psi(X) \int_{R_o}^{\infty} \phi(R) dR \quad (3)$$

and

$$N_{X_o}(R) = A\phi(R) \int_{X_o}^{\infty} \psi(X) dX , \quad (4)$$

respectively. In this case the effect of changing the sensitivity R_o (or X_o) is only to change the normalization of the distributions, but the functional form is identical to the distributions of all bursts $N_o(X)$ (or $N_o(R)$). Therefore, we can immediately test for statistical independence by comparing the distribution $N_{R_o}(X)$ or $N_{X_o}(R)$ for different sensitivities R_o or X_o with $N_o(X)$ or $N_o(R)$. Figures 2 and 3 show such a comparison for the data described in §II. The error bars given are proportional to the square root of the number of bursts in each bin (Note that the data is probably incomplete at the low end). It is evident that the curves are not parallel and that the magnitude of the slope of the distributions $N_{R_o}(X)$ shown in Figure 2 decrease with increasing radio sensitivity R_o .

This means that larger radio bursts are more likely to be accompanied by a hard X-ray burst. Alternatively, with the statistically independent assumption, one would expect the function $G(X/R_o) = N_{R_o}(X)/N_o(X)$, which is the fraction of hard X-ray bursts which are associated with a type III burst of intensity greater than R_o , to be constant for all values of R_o . However, as shown in Figure 4, this fraction increases with X indicating that the larger hard X-ray bursts are more likely to be accompanied by a type III burst.

As a qualitative measure of this behavior, we list the best fit power-law indices (excluding the incomplete bins) to the curves in Figures 2 and 3 in Table 2. The power-law index for $N_o(X)$ agrees with the well-known result for the HXRBS data (Dennis 1985 Fig. 3) and the power-law indices systematically decrease with decreasing sensitivity (increasing R_o or X_o), both for the hard X-ray and type III distributions. We conclude, therefore, that the data is inconsistent with the stochastic independence assumed in equations (3) and (4).

The question that arises is, what kind of correlation exists between these two types of emissions or parameters? We have yet to determine the functional form of the distribution $f(X, R)$ which gives rise to the observed distributions $N_{R_o}(X)$ and $N_{X_o}(R)$. In general, there are a multitude of functional forms which can describe a given set of observations. Without any loss of generality, we can write

$$f(X, R)dXdR = A\psi(X)g(Y)dXdY \quad , \quad (5)$$

where Y is an arbitrary function of X and R . Here we first analyze the simple form $Y = X/R$ discussed by PL. This form for the distribution function gives

$$N_{R_o}(X) = A\psi(X)G(X/R_o) \quad , \quad (6)$$

where

$$G(Y) = \int_0^Y g(Y')dY' \quad \text{with} \quad G(\infty) = 1 \quad (7)$$

is the fraction of bursts with hard X-ray intensity X which have radio bursts of strength $R > X/Y$. Note that $N_o(X) = A\psi(X)$. This is a useful and general way of describing

the correlation between X and R . If X and R are perfectly correlated ($X/R = Y_o$ for all events) then $g(Y) \propto \delta(Y - Y_o)$. For complete independence $g(Y)$ is featureless (e.g. a simple power-law). In other words, the “width” of the distribution $g(Y)$ provides a measure of the degree of stochastic dependence of the quantities X and R .

This distribution assumes stochastic independence of the X and Y parameters and therefore can be subjected to a similar analysis described above for the $X - R$ distribution. The distribution of the correlated events in the Y - X plane are shown in Figure 5. Also plotted is the effective instrumental cut-off at $R_o = 75$. The absence of data points in the upper left region, $Y \lesssim 10^{-1}$, $X \gtrsim 10^3$ of this figure, as well as the absence of data below the cut-off line, make these quantities appear to be strongly correlated. However, based on the occurrence rates for all flares one only expects one or two points to be in the first of the above mentioned regions so that the absence of observed flares there is not unreasonable. Due to the presence of a cut-off, the construction of the distributions $g(Y)$ or $\psi(X)$ is not straightforward. If X and Y are stochastically independent then the non-parametric method described by Petrosian (1986) is one way to construct these distributions. This method gives the cumulative functions $\Phi(X) = \int_X^\infty \psi(X') dX'$ and $G(Y)$. In Figure 6 we show the cumulative function $\Phi(X)$ for the Y parameter in the ranges $0 < Y < 0.4$ and $0.4 < Y < 6.4$. The fact that these distributions are fairly similar is an indication of the independence of X and Y . The distribution $N_{Y_o}(X) = \Phi(X)G(Y_o)$ versus X is fitted to a power-law function from which we calculate the index $d \ln \psi / d \ln X$ for various values of Y_o . The indices, given in Table 2, show no systematic variation with Y_o and within the errors agree with the power-law “index” found for all bursts ($Y_o \rightarrow \infty$). This again shows that the separation of the distribution given by equation (5) is consistent with the data.

Using the same non-parametric method we can evaluate the cumulative function $G(Y)$ (see Figure 7). The functions $\psi(X) = N_o(X)/A$ and $g(Y) = dG(Y)/dY$ then give a complete description of the distribution. This procedure, however, requires an analytic form for $G(Y)$. Except for the case of perfect correlation, there is no unique form for

$g(Y)$ or $G(Y)$. We chose a few simple functional forms with two free parameters and found the values of these parameters that best fit the data. The forms tried were gaussian, exponential, and simple power-law like forms. No satisfactory fit was obtained for the gaussian or exponential forms. The resulting best fit for the power-law like form is

$$G(Y) = 1/(1 + (Y_o/Y)^b), \quad g(Y) = bY_o^{-1}(Y/Y_o)^{b-1}/(1 + (Y/Y_o)^b)^2, \quad (8)$$

with $b = 0.82 \pm 0.07$ and $Y_o = 8 \pm 2$. This fit is shown in Figure 7. To check our method for internal consistency, we use the analytic functions $g(Y)$ and $\psi(X) \propto X^{-1.82}$ to evaluate the expected number of bursts $N_{R_o}(X)$ and compare this distribution with the data. The circles in Figure 2 show the results of this comparison for two values of R_o . Similarly, we can compute the expected distributions $N_{X_o}(R)$ of type III events,

$$N_{X_o}(R) = A \int_{X_o}^{\infty} \psi(X)g(X/R)XdX/R^2. \quad (9)$$

We see in Figure 3 that the calculated points (circles) agree with the observed histograms here as well (The lowest point doesn't fit due to the incompleteness of the radio data at low flux levels.). Therefore, the form for the bivariate distribution function of hard X-ray and type III burst intensities given by equation (5) with $g(Y)$ given by equation (8) describes the observed distribution of bursts adequately.

In order to obtain a more quantitative measure of the degree of correlation between the X-ray and type III radiations, we have repeated the same procedure with two other simple functional forms for Y : namely, $Y' = \sqrt{X}/R$, and $Y'' = X^2/R$. We find that the power-law index of $N_{Y'}(X)$ changes systematically from 1.40 (with 25 points) to 1.63 (with 132 points) as Y' is increased from 0.01 to 1.0. Furthermore, the index of 1.63 does not agree with the expected result of 1.82 for all X-ray bursts (cf. Table 2). For the choice Y'' , the power-law index of $N_{Y''}(X)$ is too large with values of 2.44 (28 points), 2.74 (70 points), and 2.55 (116 points), for $Y'' = 5, 50, \text{ and } 10^4$, respectively. Therefore, neither Y' nor Y'' appear to be stochastically independent of X and our choice of $Y = X/R$

provides a better description of the data. More elaborate functions might be chosen, such as $Y = (X - X_{th})/R$, where X_{th} may be due to another process contributing to the X-ray flux (e.g. thermal bremsstrahlung) but not to the type III emission. In this case, the distribution in X_{th} would also have to be unfolded. We feel that the data does not warrant such detailed analysis and that the thermal contribution only adds more dispersion to the data (see §IV below).

We note that our choice for the independent parameters is slightly arbitrary. Instead of X and Y we could have chosen R and Y . In fact, if X (or R) and Y were strictly statistically independent, then one could choose any function of X (or R) and Y as independent parameters. This, however, would not alter observable quantities such as the distributions $N_{R_o}(X)$, $N_{X_o}(R)$ or the values of the moments of these functions. We have repeated the calculations leading to Figures 5 through 7 using R instead of X , and Y as our parameters and have fitted the data represented in this way to the function described by equation (8) times $\psi(X) \propto X^{-1.82} = (RY)^{-1.82}$ and find $b = 0.83$ and $Y_o = 7$. These values are in agreement with the values $b = 0.82 \pm 0.07$ and $Y_o = 8 \pm 2$ found above. It is clear from this analysis that the distributions $N_o(X)$ and $N_o(R)$ should be identical. As shown in Table 2, the power-law indices (1.82 and 1.75) only differ by slightly more than one standard deviation. Therefore, the observed $N_o(R)$ distribution could be a random sample of the $N_o(X)$ distribution. Finally, we note that the ratio of X-ray to radio limiting flux $Y_{lim} = X_{lim}/R_{lim} \sim 25/75 = 1/3$ is less than the representative value Y_o of the Y parameter determined by either method. Ideal samples should have $Y_{lim} \sim Y_o$ which means that we need an improvement of a factor of 24 ($R_{lim} \sim 3$ solar flux units) in the radio data if $Y_o \sim 8$. Further lowering of R_{lim} will not increase the size of the data set significantly, or improve it, unless accompanied by proportional decreases in X_{lim} .

b) Dependence on Spectral Index

As summarized in Table 1, we have the values of the X-ray spectral index, γ , from power-law fits to the X-ray spectra for 241 of the bursts, 34 of which have been observed to

be associated with a type III burst. In this subsection, we see to what extent the spectral index effects the correlation between the hard X-ray and type III emissions.

The histogram in Figure 8 shows the fraction of hard X-ray bursts which have detected type III fluxes versus the spectral index (solid line) for $R \geq 50$. For comparison we also show (dashed line) the data from Figure 10 of Kane (1981). Both histograms show that a larger fraction of harder (smaller γ) X-ray bursts produce type III bursts. This effect is much less pronounced in the new data. In fact, a χ^2 -test gives $\chi^2 = 4.6$ (with 7 degrees of freedom) and therefore a probability of 0.70 that the χ^2 found from a parent distribution which is uniform would be this large or larger. Hence, we cannot exclude the possibility that there is not a correlation. This presumably is not true for Kane's (1981) results and we do not know the reason for this difference. To determine whether or not the spectral index dependence that we do see is due to selection effects, such as correlation of X-ray intensity with spectral index, we have performed the following test. We binned all X-ray bursts with known spectral index (241 of them) by spectral index. Since the probability that an X-ray event of strength X is associated with a type III burst is known (cf. Figure 2), we can compute the expected number of type III associated events for each bin. This is found by summing the probability of type III association for each individual event over all X-ray events in the bin. The result of this calculation is shown in Figure 9 along with the observed number of hard X-ray bursts (with known spectral indices) associated with a type III burst. We see that for $\gamma > 4.5$ the number of associated bursts is equal to that expected from the total distribution while for $\gamma < 4.5$ the number of associated bursts is twice that expected. In this case, we find $\chi^2 = 3.0$ (8 degrees of freedom) which gives a higher probability (0.93) that this χ^2 could have come from a distribution which is uniform in spectral index. This indicates that some sampling bias exists. In order to conclude that the increased correlation between hard X-rays and type III emission for harder X-ray spectra is a real effect, a larger sample is needed.

IV. Discussion

We have shown that the observed distribution of the type III and hard X-ray emission from solar flares can be described by a bivariate distribution with independent parameters the X-ray intensity and the ratio of the X-ray to type III intensities. This implies a correlation between these two types of emission. However, this correlation is stochastic as demonstrated by the large range (or “width”) of the distribution $g(Y)$ in equation (8). Strictly speaking, both the average value and mean dispersion of Y for this distribution diverges. This, however, is an artifact of the simple distribution chosen here and can be remedied by the introduction of additional parameters. The important conclusion we draw from this is that a typical value for the ratio Y is the quantity $Y_o \sim 8$ and the range of Y is even greater than Y_o and can be as large as $10^2 Y_o \sim 10^3$. We now discuss the meaning of these results and the results from consideration of the spectral index dependence in the frame work of models for the impulsive phase of the flare and for the two types of radiation under consideration here.

a) Nature of the Correlation

We first consider the correlation we have found between the X-ray and type III emissions and in particular the appropriateness of the choice $Y = X/R$ as a stochastic parameter.

The X-rays of energies $20 \sim 100$ keV are produced mainly by bremsstrahlung of electrons with comparable energies. Three distinct models have been advanced to explain the solar hard X-ray emission by electrons, the thick-target, thin-target, and thermal models (trap plus precipitation models are classified as thick-target here because the X-ray production is via thick-target bremsstrahlung of the precipitating electrons). In both the thick and thin target models, nonthermal electrons produce the impulsive X-ray bursts and the strength of the burst is proportional to, n_x , the number of nonthermal electrons. In thermal models, the level of X-rays produced is proportional to n_x^2 . Since the corona is

optically thin to photons in this energy range, the observed radiation is also proportional to n_x (nonthermal) or n_x^2 (thermal). Although there is often some contribution from thermal emission, the impulsive X-ray bursts are most likely due to nonthermal electrons.

The relationship between the number of type III producing electrons, n_{III} , and the intensity of type III bursts is more complicated. Type III bursts are produced by nonthermal electrons with energies $E \sim 30$ keV ($\beta \sim 1/3$) which develop a positive slope in their velocity distribution as they propagate. This situation is unstable to the generation of longitudinal plasma waves (Langmuir waves) with frequency near the local plasma frequency. These waves don't propagate or escape the plasma, so that a mechanism for conversion of these waves to escaping radiation is needed. There are two processes which are believed to occur. The coalescence of two longitudinal waves to form a transverse wave at twice the plasma frequency (second harmonic emission) and the scattering of a longitudinal wave off ion-acoustic turbulence into a transverse wave with frequency near the local plasma frequency (fundamental emission). To find the relation between n_{III} and the intensity of type III radiation we must first relate n_{III} to the level of plasma turbulence generated, W_l , and then relate this to the intensity, R , of type III radiation.

The first of these relations is simple $W_l \propto n_{III}$. The relationship between the turbulence level and the intensity of type III radiation was discussed by Smith and Spicer (1979). For second harmonic emission they showed that $R \propto W_l$ when optically thick and $R \propto W_l^2$ for optically thin sources. Therefore, $R \propto n_{III}$ or $R \propto n_{III}^2$ for second harmonic emission from an optically thick or optically thin source, respectively. They also showed that $R \propto W_l$ for optically thin fundamental emission. For optically thick sources the fundamental emission depends on the ratio of Langmuir turbulence to ion-acoustic turbulence. However, the second harmonic emission is usually dominant for type III bursts and for solar type III bursts the source is generally optically thick. So that for most type III bursts $R \propto W_l \propto n_{III}$.

Combining the results for X-ray and type III emission, we see that for the most

likely situation where impulsive hard X-rays are produced by nonthermal electrons and the type III burst is second harmonic emission from an optically thick source the quantity $Y = X/R \propto n_x/n_{III}$. Therefore, if this ratio is independent of X or R then Y is a good variable with which to characterize the correlation of X-ray and type III bursts. Other situations are of course possible and would lead to other parameterizations. For example, for nonthermal models ($X \propto n_x$) with optically thin second harmonic type III emission ($R \propto n_{III}^2$) parameterization in terms of $Y'' = X^2/R \propto (n_x/n_{III})^2$ would be more natural. Or, if X-rays are produced by thermal bremsstrahlung ($X \propto n_x^2$) and type III radiation by optically thick second harmonic emission, then the parameter $Y' = \sqrt{X}/R \propto n_x/n_{III}$ would be the natural parameter if $n_{III} \propto n_x$. For these cases, however, there may not be any correlation between n_x and n_{III} so that one would expect no correlation between X and R and a distribution function as described in connection with equations (3) and (4). As shown in the previous section, all of these other possibilities are less likely than the parameterization in terms of X and $Y = X/R$, corresponding to nonthermal X-rays and optically thick second harmonic type III emission.

Thus, we can conclude that the ratio $Y = X/R$ is proportional to the ratio $Y_e = n_x/n_{III}$ of the number of X-ray to type III producing electrons; $Y = \eta Y_e$. Part of the large (three or four orders of magnitude) observed dispersion in the value of Y is due to the dispersion of the proportionality “constant” η which depends on the properties of the flare plasma, especially those determining the level of plasma turbulence W_l . We estimate η to be 10^{-1} to 10^{-3} based on the relation between n_x and X which is straightforward (cf. Hoyng, Brown, and Van Beek 1976) and on the relation between n_{III} and R which is very model dependent. We have used the relations given by Smith and Spicer (1979) and assumed a velocity of $c/3$ for the electrons, a range for plasma temperature of 10^6 to 10^7 , and efficiency of plasma wave generation of 0.1 to 1. Equally important in the dispersion of Y is the variation of the ratio Y_e from flare to flare. The ratio Y_e depends on a number of factors related to the acceleration mechanism and the transport of the

accelerated electrons in the solar atmosphere. The most important among these factors is the ratio of the number of accelerated electrons which end up on open field lines (lines extending to the upper corona and/or the interplanetary medium) to those on closed field lines, which we denote by ϵ .

All electrons on the closed field lines and a fraction f_x of those on the open field lines contribute to the X-rays while the rest contribute to the type III emission. (We assume that X-ray emitting electrons have a negligible contribution to the type III emission and vice versa). Thus, the ratio $Y_e = (1 + \epsilon f_x)/\epsilon(1 - f_x)$. The ratio f_x in turn depends on two factors. The first of which is the fraction of the electrons on the open field lines directed outward from the sun, f_{up} , which is determined by the pitch angle distribution of the accelerated electrons (e.g. $f_{up} = 1/2$ for isotropic pitch angle distribution). Due to pitch angle diffusion and field convergence a fraction f_{ref} of the down going electrons are reflected back so that $f_x = (1 - f_{ref})(1 - f_{up})$ and

$$Y_e = \frac{1 + \epsilon(1 - f_{ref})(1 - f_{up})}{\epsilon(f_{up} + f_{ref} - f_{ref}f_{up})} , \quad (10)$$

which is the same as equation (17) of PL with different notation.

First we note that based on our estimated range of values for η , a typical observed ratio $Y = Y_o$ requires the value $Y_{eo} \sim Y_o/\eta \sim 10^{3\pm 1}$. The important point here is that despite the large uncertainty we require $Y_e \gg 1$ even for those flares with minimal X-ray emission having $Y \sim 1$. According to equation (10), this can be the case if either $\epsilon \ll 1$ or $(f_{up} + f_{ref}) \ll 1$ or both. It can be shown that within a factor of two this expression can be simplified as

$$Y_e \approx \frac{1 + \epsilon}{\epsilon(f_{ref} + f_{up})} , \quad (11)$$

which should be sufficient for our discussion considering the large uncertainties in the other parameters. The large dispersion in the value of Y can then be easily accommodated by the dispersion in the three parameters in equation (11). Of these, ϵ and f_{up} depend on

the acceleration process and the geometry of the magnetic field ($0 < \epsilon < \infty$, $0 < f_{up} < 1$) while f_{ref} depends on the transport effects and is expected to be small ($f_{ref} \ll 1$).

Another contribution to outgoing type III producing electrons may come from possible diffusion across the magnetic field lines (from closed to open field lines) as in the model proposed by Emslie and Vlahos (1980, hereafter EV). In the general version of the model, Y_e is given by equation (10) or (11) with the addition in the denominator of another term f_{diff} which is the fraction of electrons in the closed loop that diffuse to the open field lines with pitch angles so that they stream outward from the sun. In the version of this model proposed by EV, all particles are on closed field lines so that $\epsilon = 0$ and

$$Y_e \approx f_{diff}^{-1} . \quad (12)$$

In general, f_{diff} is expected to be small so that $Y_e \gg 1$ as required, but the distribution of f_{diff} (the values of the expected average and rms values) is not explicitly specified by the model and difficult to predict.

Finally, let us consider a third model for the production of type III radiation proposed by Sprangle and Vlahos (1983, hereafter SV). In this model, the primary electrons which are accelerated in a closed loop with a converging magnetic field reflect to acquire a loss cone distribution. This electron distribution is unstable and results in cyclotron maser emission. The emitted radiation then escapes the closed field lines of the loop and accelerates secondary electrons on open field lines. This model is able to account for short time delays between peaks in the type III emission relative to peaks in the X-ray emission (Dennis *et al.* 1984). SV show that the number of accelerated electrons is proportional to the magnitude of the loss cone, and therefore to the number of reflected electrons, times factors related to the efficiency of the secondary acceleration process. Since the number of reflected electrons is proportional to n_x , this model also agrees with the Y parameterization that we used and predicts a value of Y_e given by equation (10) or (11) with addition of another term $\propto f_{ref}$ in the denominator for the contribution to n_{III} by the secondary

process. Of course, as in the EV model, this model is of interest when $\epsilon = 0$. So that in the simplest form of the model $Y_e \propto f_{ref}^{-1}$. As we shall see below $f_{ref} \ll 1$ and $Y_e \gg 1$ as expected. However, again determination of the average or rms value of Y_e is difficult in this model.

b) Dependence on Spectral Index

The discussion above shows that most model predictions agree with the observed distribution and its parameterization in terms of X and $Y = X/R$. We now consider the dependence of the X-ray and type III correlation on the X-ray spectral index. In general, for nonthermal models there is a simple relation between the X-ray spectral index γ and the electron spectral index δ . In particular, for the thick target models considered here in their simplest form, $\gamma = \delta - 1$. This relation is not exact and depends on the parameters of the model (see Leach and Petrosian 1983, or Leach 1984), but for our purposes here it is sufficient to note that as δ increases γ increases so that the observed correlation between the distribution and γ (if any) reflects correlation between δ and Y_e .

As shown in the previous section, the new data does not show the strong dependence on spectral index found by Kane (1981), so that the degree of the correlation is not well determined. However, we believe that bursts with harder X-ray spectra are more likely to also have type III emission. This can be described mathematically by making Y_o (or b) to be a function of spectral index. If we take b to be independent of spectral index then for each spectral index bin the fraction of bursts with type III emission is

$$f(\gamma) = \frac{\int_{X_o}^{\infty} \psi(X) G[X/R_o Y_o(\gamma)] dX}{\int_{X_o}^{\infty} \psi(X) dX} . \quad (13)$$

For $\psi(X) \propto X^{-\alpha}$ and $G(Y)$ given by equation (8) this reduces to

$$f(\gamma) = Z_o^{\alpha-1} / (\alpha - 1) \int_{Z_o}^{\infty} dZ Z^{b-\alpha} / (1 + Z^b) , \quad (14)$$

where $Z_o = Y_{lim}/Y_o(\gamma)$. As noted above $Y_{lim} \sim 1/3 \ll Y_o$ so that $Z_o \ll 1$, in which case, to within some slowly varying logarithmic factor, the variation with spectral index

of this fraction can be approximated as $f(\gamma) \approx [Y_{lim}/Y_o(\gamma)]^b$. Our results and those by Kane (1981) shown in Figure 8 indicate $f(\gamma) \approx \gamma^{-1}$ and γ^{-3} , respectively. If we assume $f(\gamma) \approx \gamma^{-2}$ and neglect the slight difference between the exponent b and unity the data would require $Y_o(\gamma) \propto \gamma^2$. This is a very approximate relation that implies $Y_e \propto \delta^2$, a requirement that the models must satisfy. If instead of Y_o we assume b to be a function of γ then the above approximation is still valid and $\ln f(\gamma) = b(\gamma) \ln(Y_{lim}/Y_o)$. Thus, an observed $f(\gamma) \propto \gamma^{-a}$ can be described by $b = b_o - a \ln(\gamma/\gamma_o)$, where b_o is the value of b at γ_o . In what follows we consider the case that b is constant and $Y_o = Y_o(\gamma)$.

In the simple nonthermal model it is evident from equation (11) that we require $\epsilon \neq 0$ otherwise there will not be any type III emission. Furthermore, in its simplest form this model does not require or predict dependence on the spectral index δ for this parameter or for f_{up} which is a moment of the pitch angle distribution of the accelerated electrons. Then, as proposed by PL, the only dependence on δ will arise from the variation of f_{ref} with δ . As also shown by PL, there is considerable variation of f_{ref} with δ especially for models with electrons beamed primarily downward $f_{up} \rightarrow 0$ so that $Y_e \propto f_{ref}^{-1}$. From Table I of PL we see that for this case (their parameter $\alpha_0^2 < 1$) f_{ref} increases more rapidly than linearly, so that the trend agrees roughly with the above requirement.

On the other hand, if the pitch angle distribution of the accelerated electrons is isotropic $f_{up} = 1/2$, then we require $\epsilon \ll 1$ so that $Y_e \propto (1 + 2f_{ref})^{-1}$. Since, in general $f_{ref} \ll 1$, this predicts a slower variation. In addition, for an isotropic pitch angle distribution the above mentioned Table of PL shows a slower variation of f_{ref} with δ . Consequently, we expect very little variation of Y_e with δ and Y_o (or $f(\gamma)$) with γ . Note that for both of these cases the dependence on δ is weakened with increasing magnetic field convergence.

For a quantitative comparison of these models with the data we assume that the spectral indices are related as in the simple thick-target model, $\gamma = \delta - 1$, and choose ϵ/η so that $Y_o = 8$ for the median spectral index $\gamma = 4$. This means that $\eta Y_e(\delta = 5) = 8$.

The fraction $f(\gamma)$ is computed using equation (13) with $Y_o(\gamma)$ given by equation (10). The model parameters are listed in Table 3 and the corresponding $f(\gamma)$'s are shown in Figure 10 for comparison with the data. We find that the calculated fractions agree with the above qualitative discussion. The isotropic models show very little variation with spectral index while the beam models fit the data well, suggesting that the pitch angle distribution of accelerated electrons is beamed toward the sun.

In the EV model (with $\epsilon = 0$) $Y_e \propto f_{diff}^{-1}$. It is not clear why f_{diff} would be dependent on spectral index δ . However, since higher energy particles penetrate to higher depths below the transition region and if the diffusion rate across the field lines also increases with depth then bursts with harder spectra (lower δ) will have larger f_{diff} , a lower Y_e or Y_o , and therefore a larger fraction $f(\gamma)$ associated with type III emission.

In the SV model, the strength of the loss cone determines the strength of the type III emission. Since the bulk of the strength of the loss cone comes from lower energy electrons and since the loss cone is produced by mirroring before much collisional energy loss occurs, we expect little dependence on the spectral index. For this model the field convergence is strong so that f_{ref} approaches unity with very weak dependence on δ .

Clearly we require more spectral index information before such observations can be used to distinguish between the various possibilities described above.

V. Summary

We have analyzed a large number of hard X-ray events which occurred during the maximum of the 21st solar cycle in order to study their correlation with type III bursts. From our analysis, we found that the distribution of occurrences of hard X-ray bursts which are correlated with a type III radio burst is significantly different than the distribution of all hard X-ray bursts, which is consistent with results found by previous authors. We were able to show that this result is consistent with the assumption that the hard X-ray and type III intensities are somewhat correlated. A bivariate distribution function of the

burst intensities was fit to the data. From this distribution we determined that the typical ratio of X-ray intensity to type III intensity is $Y \sim 8$ and that the ratio of the number of X-ray producing electrons to type III producing electrons is in the range $Y_e \sim 10^2$ to 10^4 . However, there is a large dispersion in the ratio of peak X-ray intensity to type III intensity.

Three models that have been proposed to explain the relation between hard X-ray and type III producing electrons were examined in the context of these observations. All models predict that $Y \propto Y_e$ and that it is independent of both X-ray and type III intensity which agrees with the data. The important differences in the models are whether or not both electron populations are accelerated simultaneously and whether the correlation between hard X-rays and type III radiation increases for harder X-ray bursts. The data indicate that this correlation increases slightly with decreasing X-ray spectral index. The increased correlation of X-ray and type III events with decreasing photon spectral index is explained in the model of PL by the increase in the fraction of reflected electrons for harder electron spectra suggesting that reflected electrons play a role in type III bursts. The observed variation with spectral index is best fit by models in which the accelerated electrons, especially those on open field lines, are beamed toward the sun. More data is needed to further quantify this correlation so that the predictions of the impulsive phase models can be further tested. However, this also requires more detailed acceleration models so that the spectral index dependence of the ratio Y_e can be determined.

Acknowledgments

We would like to thank Dr. B.R. Dennis for providing the HXRBS data and Dr. A. O. Benz for providing the radio data. We are grateful to Dave Caditz for making some statistical analysis subroutines available, to Jim McTiernan for useful discussions, and to Katrina Lane who aided us in the initial gathering and analysis of the data. We acknowledge support of this work by National Aeronautics and Space Administration grant NSG-7092 and National Science Foundation grant ATM 8705084.

Table 1

Summary of hard X-ray, type III data, and the correlated events.

Hard X-Ray Bursts	
All events:	
Total number of bursts	3490
Number of bursts with known spectral index	241
Correlated events:	
Total number of bursts	134
Number of bursts with known spectral index	34
Type III Bursts	
Total number of bursts	944
Number of correlated bursts	134

Table 2

Power-law fit to the functions $N_{R_o}(X)$, $N_{X_o}(R)$, and $N_{Y_o}(X)$.

$N_{R_o}(X)$				$N_{X_o}(R)$				$N_{Y_o}(X)$			
R_o	n	α	$\Delta\alpha$	X_o	n	α	$\Delta\alpha$	Y_o	n	α	$\Delta\alpha$
0	3490	1.82	0.02	0	944	1.75	0.04	∞	3490	1.82	0.02
75	126	1.39	0.06	20	132	1.54	0.08	6.4	113	1.82	0.07
150	93	1.33	0.06	40	101	1.48	0.09	1.6	100	1.78	0.08
300	63	1.30	0.07	80	76	1.44	0.10	0.4	59	1.98	0.17
600	38	1.27	0.09	320	36	1.37	0.13	0.1	24	1.95	0.25

n is the number of points in the distribution.

α is the power-law index such that $f(z) \propto z^{-\alpha}$.

Table 3

PL Model Parameters

model	f_{up}	r_m	$\log(\epsilon/\eta)$
B1	0	1	2.90
B5	0	5	0.37
I1	$\frac{1}{2}$	1	-0.62
I5	$\frac{1}{2}$	5	-0.67

r_m is the factor by which the magnetic field increases from the injection point to the transition region.

References

- Dennis, B.R. 1985, *Solar Phys.*, **100**, 465.
- Dennis, B.R., Benz, A.O., Ranieri, M., and Simnett, G.M. 1984, *Solar Phys.*, **90**, 383.
- Dennis, B.R. *et al.* 1988, *The Hard X-Ray Burst Spectrometer Event Listing 1980-1987*, NASA Technical Memorandum 4036.
- Emslie, A.G. and Vlahos, L. 1980, *Ap. J.*, **242**, 359.
- Hoyng, P., Brown, J.C., and Van Beek, H.F. 1976, *Solar Phys.*, **48**, 197.
- Kane, S.R. 1981, *Ap. J.*, **247**, 1113.
- Kane, S.R., Pick, M., and Raoult, A. 1980, *Ap. J. (Letters)*, **241**, L113.
- Kane, S.R., Benz, A.O., and Treumann, R.A. 1982, *Ap. J.*, **263**, 423.
- Kane, S.R. *et al.* 1980, in P.A. Sturrock (ed.), *Solar Flares*, (Boulder: Colorado Assoc. Univ. Press), p.187.
- Leach, J. 1984, "*The Impulsive Hard X-rays from Solar Flares*", Stanford University (Ph.D. Thesis).
- Leach, J. and Petrosian, V. 1983, *Ap. J.*, **269**, 715.
- Petrosian, V. and Leach, J. 1983, *Solar Phys.*, **87**, 165.
- Petrosian, V. 1986, in G. Giuricin (ed.), *Structure and Evolution of Active Galactic Nuclei*, (Dordrecht [Netherlands]: Reidel), p. 353.
- Ramaty, R. *et al.* 1980, in P.A. Sturrock (ed.), *Solar Flares*, (Boulder: Colorado Assoc. Univ. Press), p.117.
- Raoult, A., Pick, M., Dennis, B.R., and Kane, S.R. 1985, *Ap. J.*, **299**, 1027.
- Simnett, G.M. and Benz, A.O. 1986, *Astr. Ap.*, **165**, 227.
- Smith, D.F. and Spicer, D.S. 1979, *Solar Phys.*, **62**, 359.
- Sprangle, P., and Vlahos, L. 1983, *Ap. J. (Letters)*, **273**, L95.

Figure Captions

- Fig. 1. Distribution of the correlated events in the R-X plane.
- Fig. 2. Distribution of all HXRBS events $N_o(X)$ and $N_{R_o}(X)$ for $R_o = 75$ and 300 with the $R_o = 300$ histogram reduced by a factor of ten for clarity. The solid lines show the best fit power-law for each of the histograms. The circles are the values calculated using the best fit to the function $G(Y)$.
- Fig. 3. Same as Figure 2 except for type III distributions $N_o(R)$ and $N_{X_o}(R)$ for $X_o = 40$ and 320 with the $X_o = 320$ histogram reduced by a factor of ten for clarity.
- Fig. 4. Fraction of X-ray events correlated with a type III event for minimum radio intensities of $R_o = 75$ and 300 solar flux units. The $R_o = 300$ histogram is reduced by a factor of ten for clarity.
- Fig. 5. Distribution of the correlated events in the Y-X plane. Also shown is the instrumental cut-off at $R=75$.
- Fig. 6. Cumulative distribution $\Phi(X)$ for $0 < Y < 0.4$ and $0.4 < Y < 6.4$ obtained using the non-parametric method with the $0 < Y < 0.4$ curve reduced by a factor of two for clarity. Also shown is the best fit power-law for each of the distributions.
- Fig. 7. The cumulative distribution, $G(Y)$, obtained using the non-parametric method along with the best fit curve equation (8).
- Fig. 8. Ratio of correlated events to total HXRBS events as a function of photon spectral index (solid). Also depicted are the results from Figure 10 of Kane (1981) (dashed). The power-law functions $f \propto \gamma^{-1}$ and γ^{-3} are also shown.
- Fig. 9. The number of observed correlated bursts (solid) and the expected number of correlated bursts (dashed) as a function of X-ray spectral index.
- Fig. 10. The observed fraction of correlated events as a function of spectral index $f(\gamma)$ is shown (histogram) along with the predictions of the PL models of Table 3. Models B1 and I1 are shown as solid lines while B5 and I5 are dashed.

Addresses

Russell J. Hamilton

323 ERL

Center for Space Science and Astrophysics

Stanford University

Stanford, CA 94305

Vahé Petrosian

304 ERL

Center for Space Science and Astrophysics

Stanford University

Stanford, CA 94305

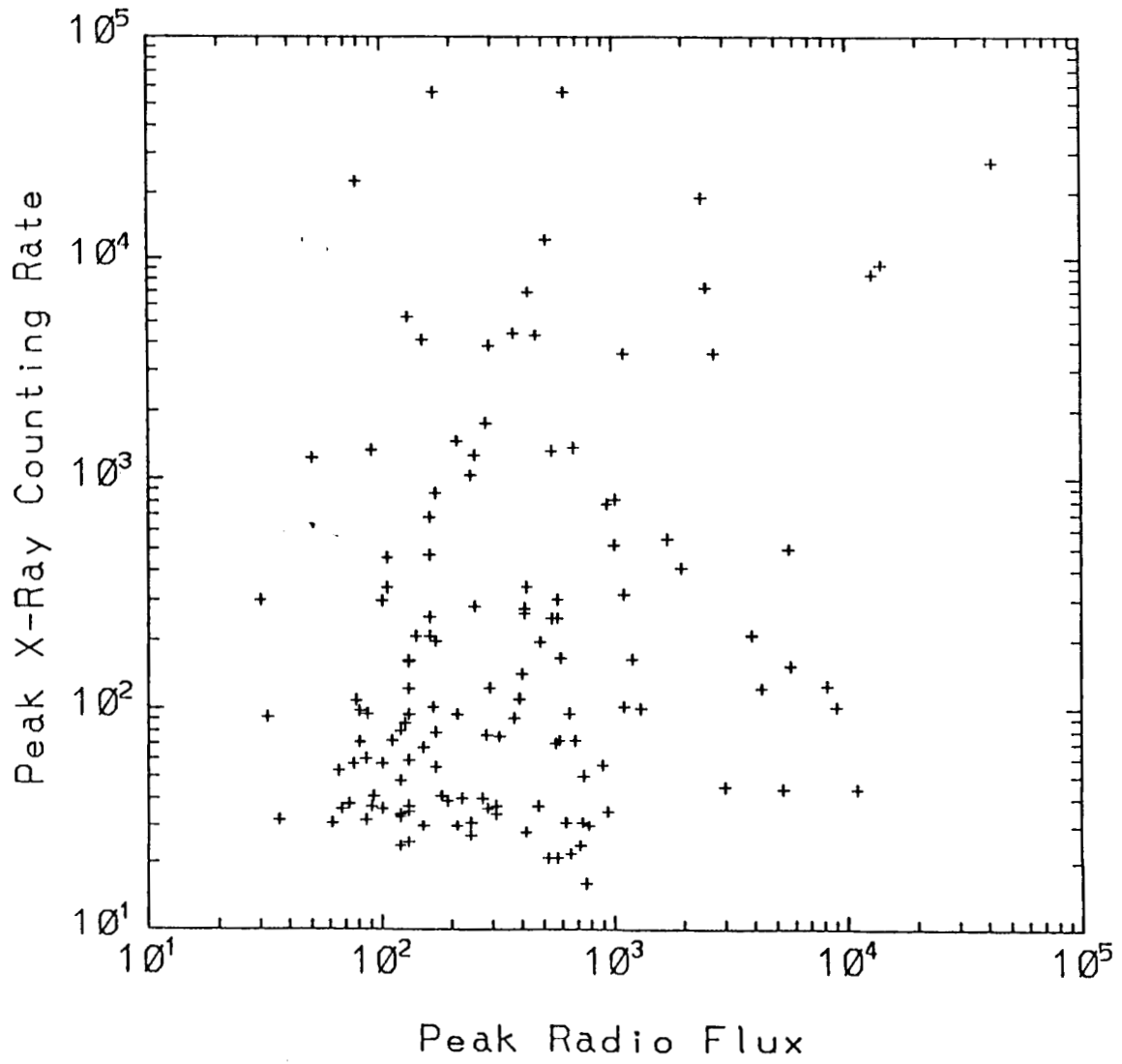


Fig. 1. Distribution of the correlated events in the R-X plane.

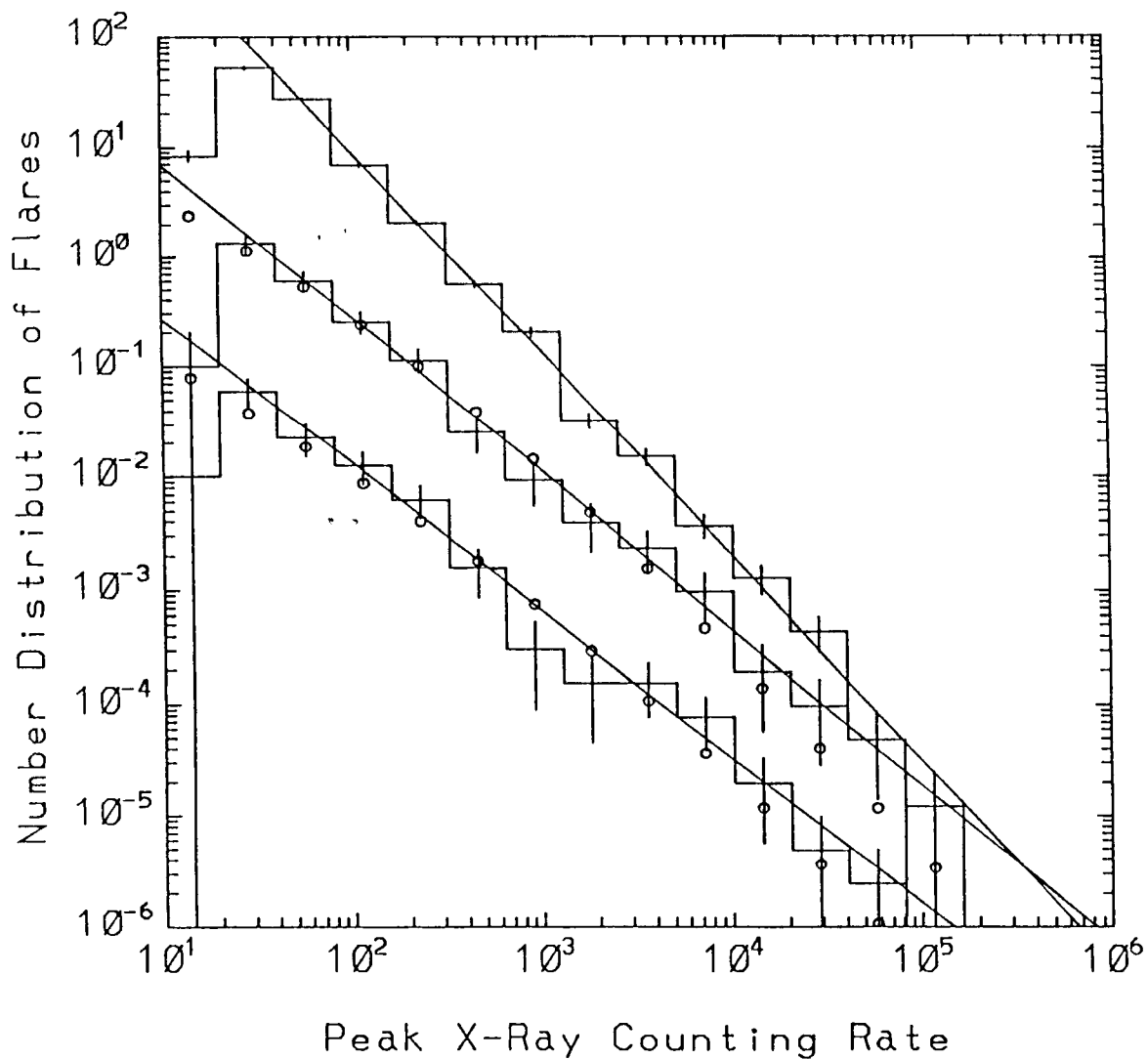


Fig. 2. Distribution of all HXRBS events $N_o(X)$ and $N_{R_o}(X)$ for $R_o = 75$ and 300 with the $R_o = 300$ histogram reduced by a factor of ten for clarity. The solid lines show the best fit power-law for each of the histograms. The circles are the values calculated using the best fit to the function $G(Y)$.

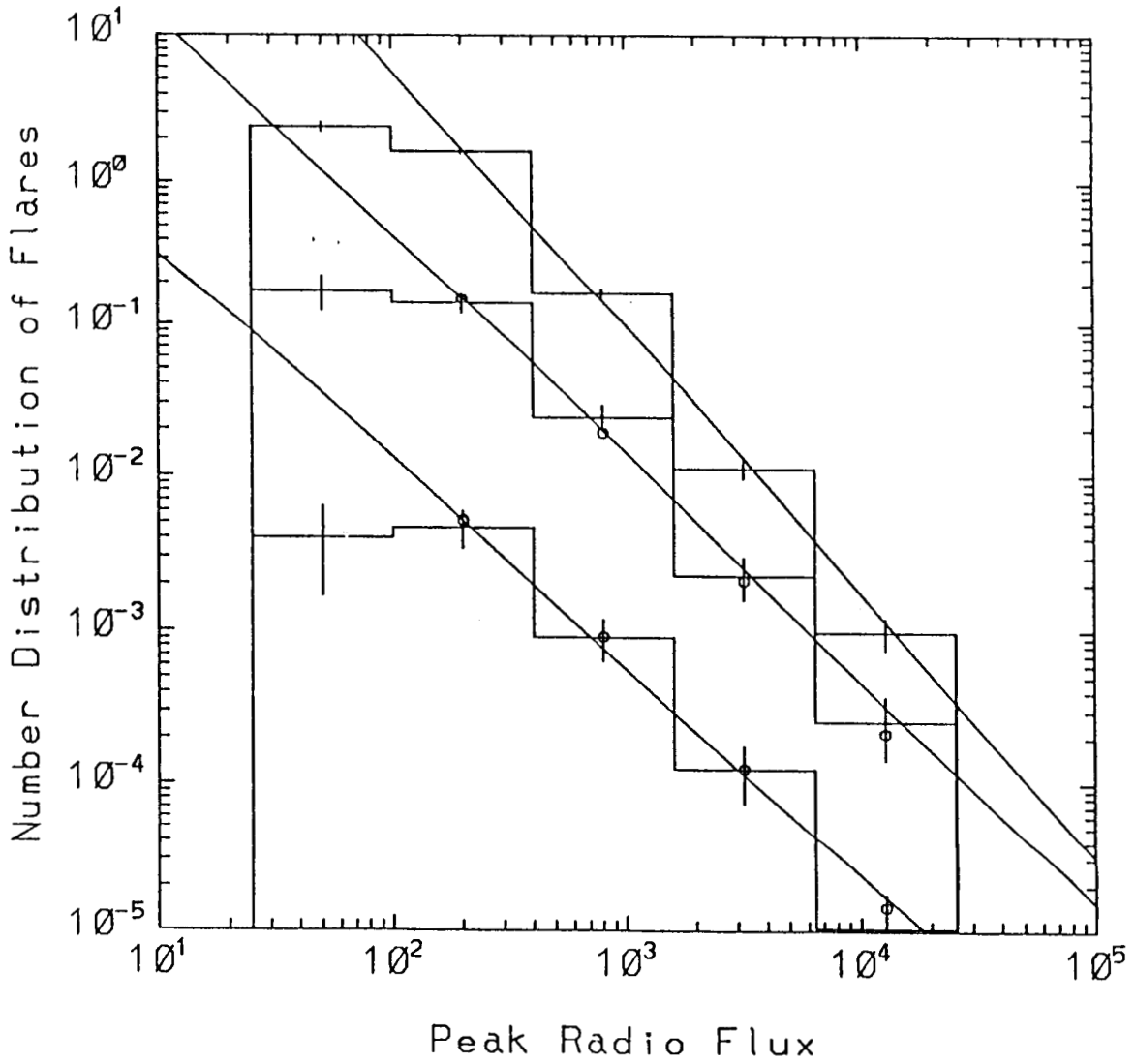


Fig. 3. Same as Figure 2 except for type III distributions $N_o(R)$ and $N_{X_o}(R)$ for $X_o = 40$ and 320 with the $X_o = 320$ histogram reduced by a factor of ten for clarity.

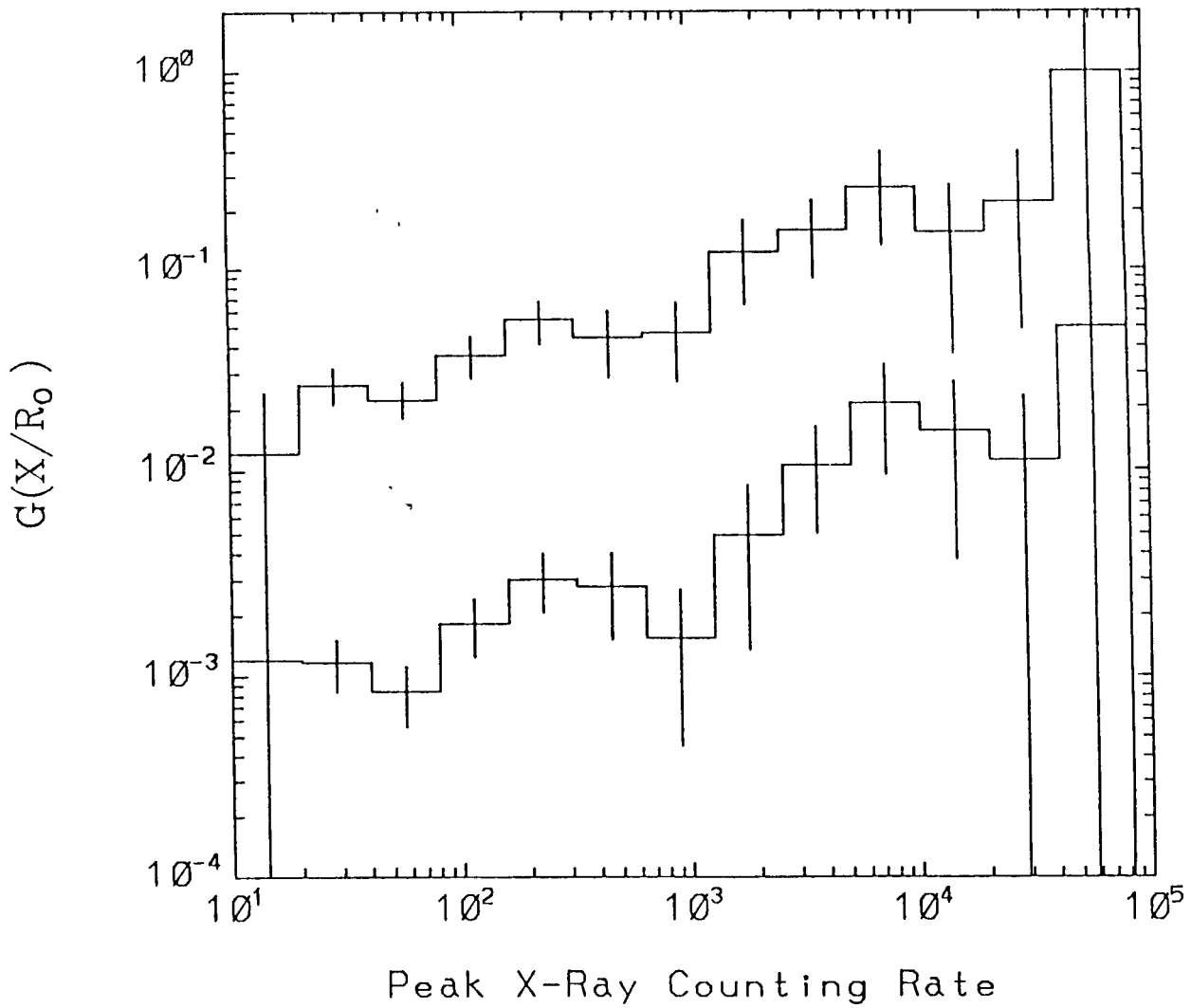


Fig. 4. Fraction of X-ray events correlated with a type III event for minimum radio intensities of $R_0 = 75$ and 300 solar flux units. The $R_0 = 300$ histogram is reduced by a factor of ten for clarity.

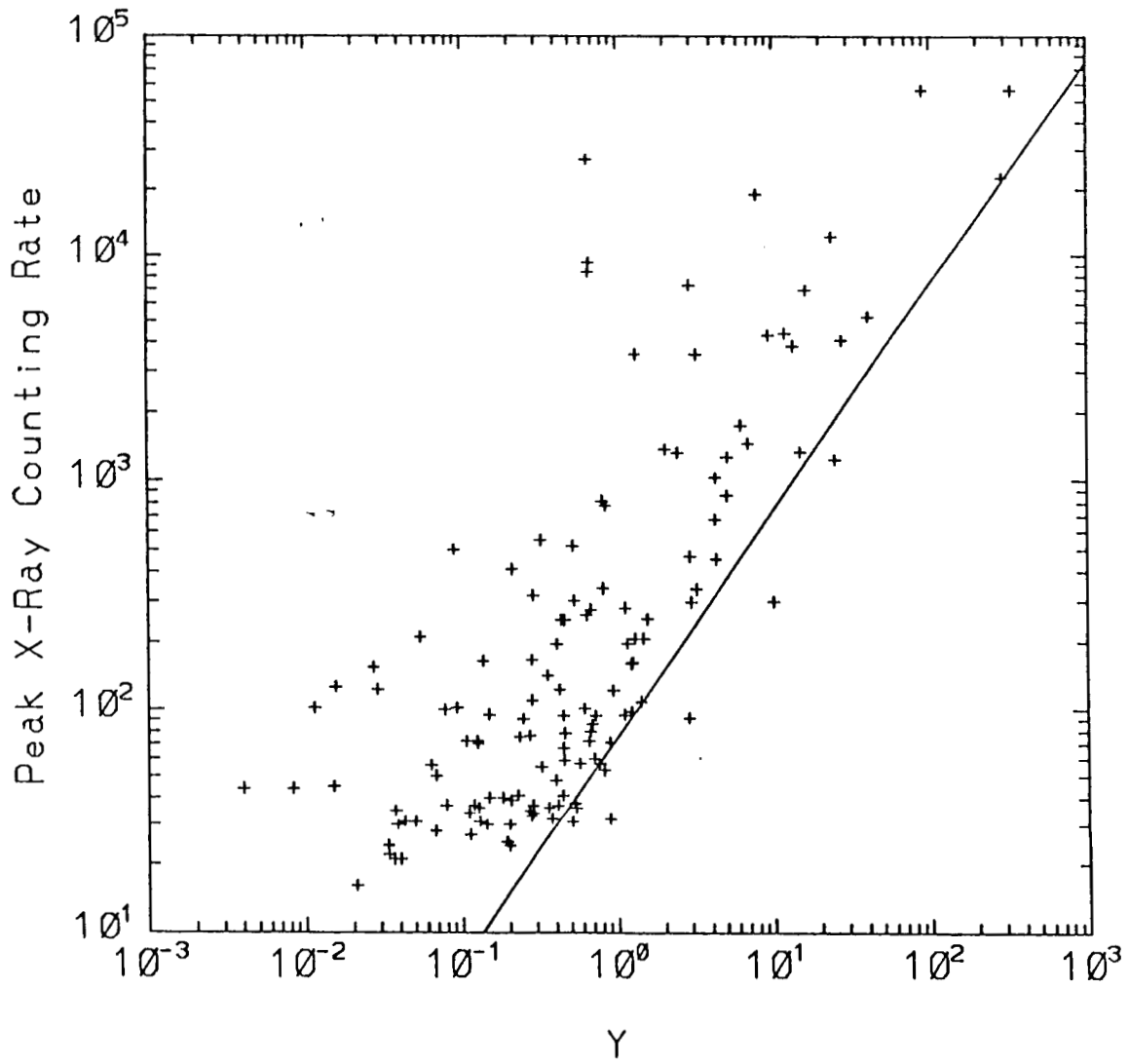


Fig. 5. Distribution of the correlated events in the Y-X plane. Also shown is the instrumental cut-off at $R=75$.

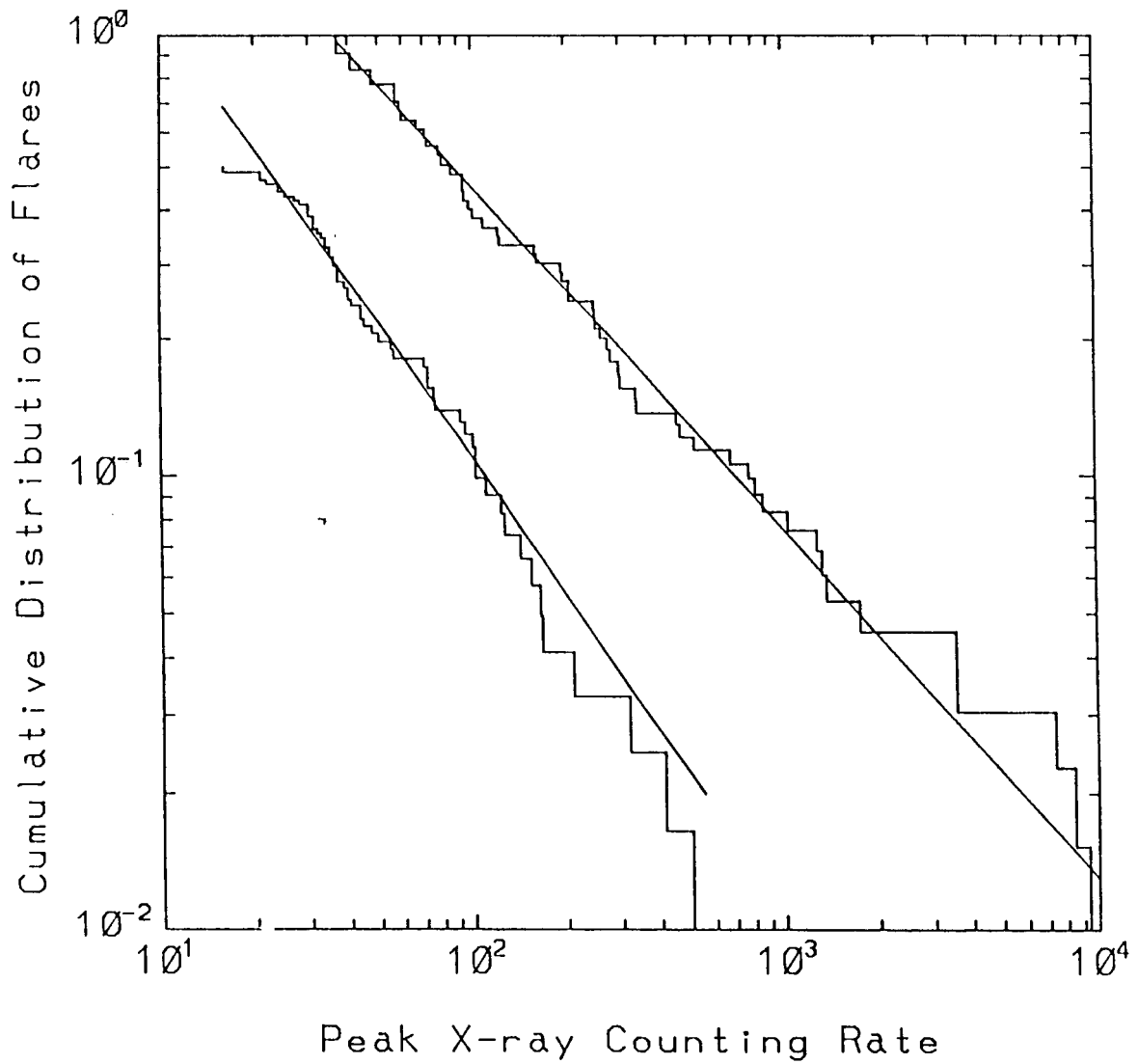


Fig. 6. Cumulative distribution $\Phi(X)$ for $0 < Y < 0.4$ and $0.4 < Y < 6.4$ obtained using the non-parametric method with the $0 < Y < 0.4$ curve reduced by a factor of two for clarity. Also shown is the best fit power-law for each of the distributions.

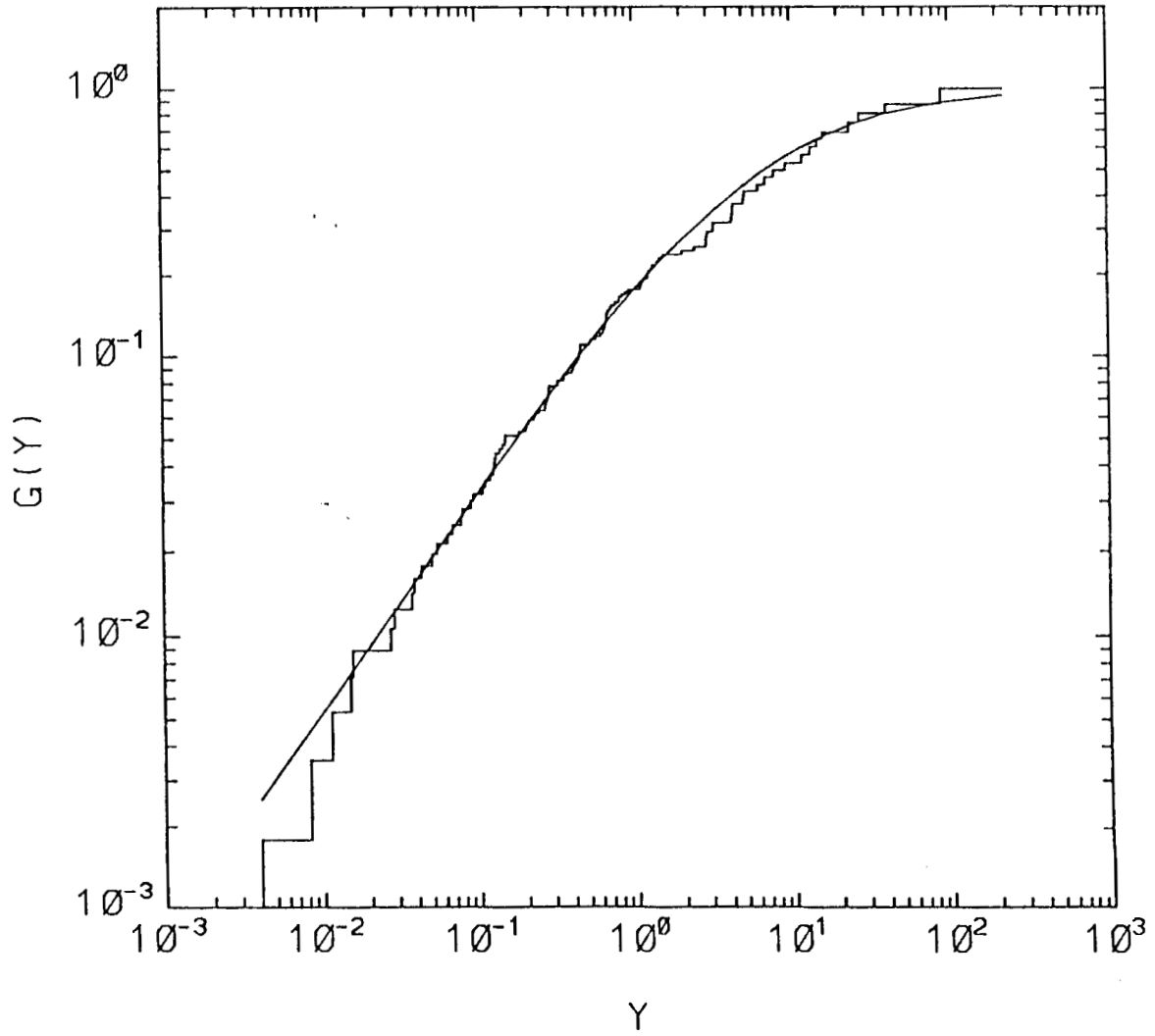


Fig. 7. The cumulative distribution, $G(Y)$, obtained using the non-parametric method along with the best fit curve equation (8).

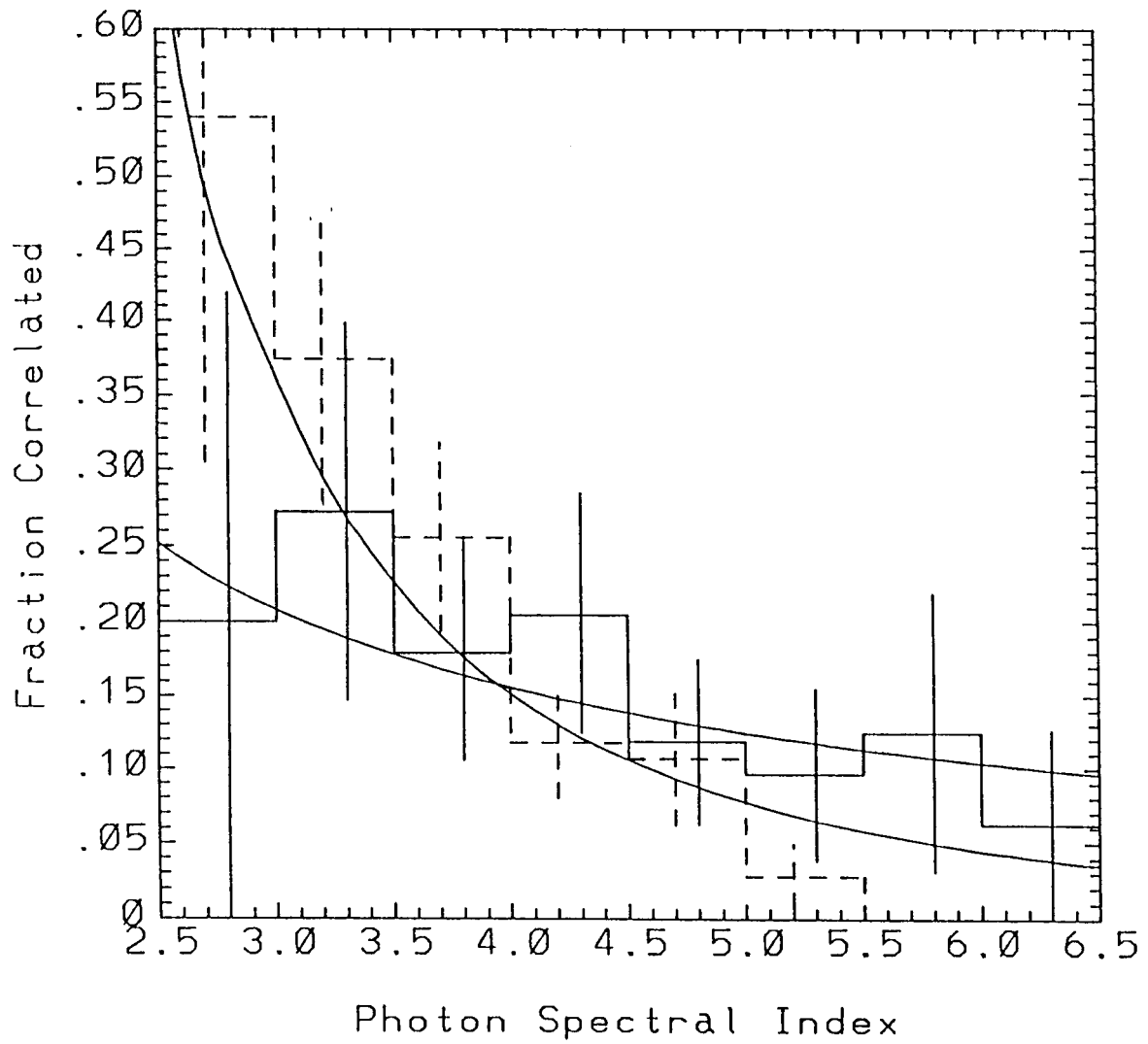


Fig. 8. Ratio of correlated events to total HXRBS events as a function of photon spectral index (solid). Also depicted are the results from Figure 10 of Kane (1981) (dashed). The power-law functions $f \propto \gamma^{-1}$ and γ^{-3} are also shown.

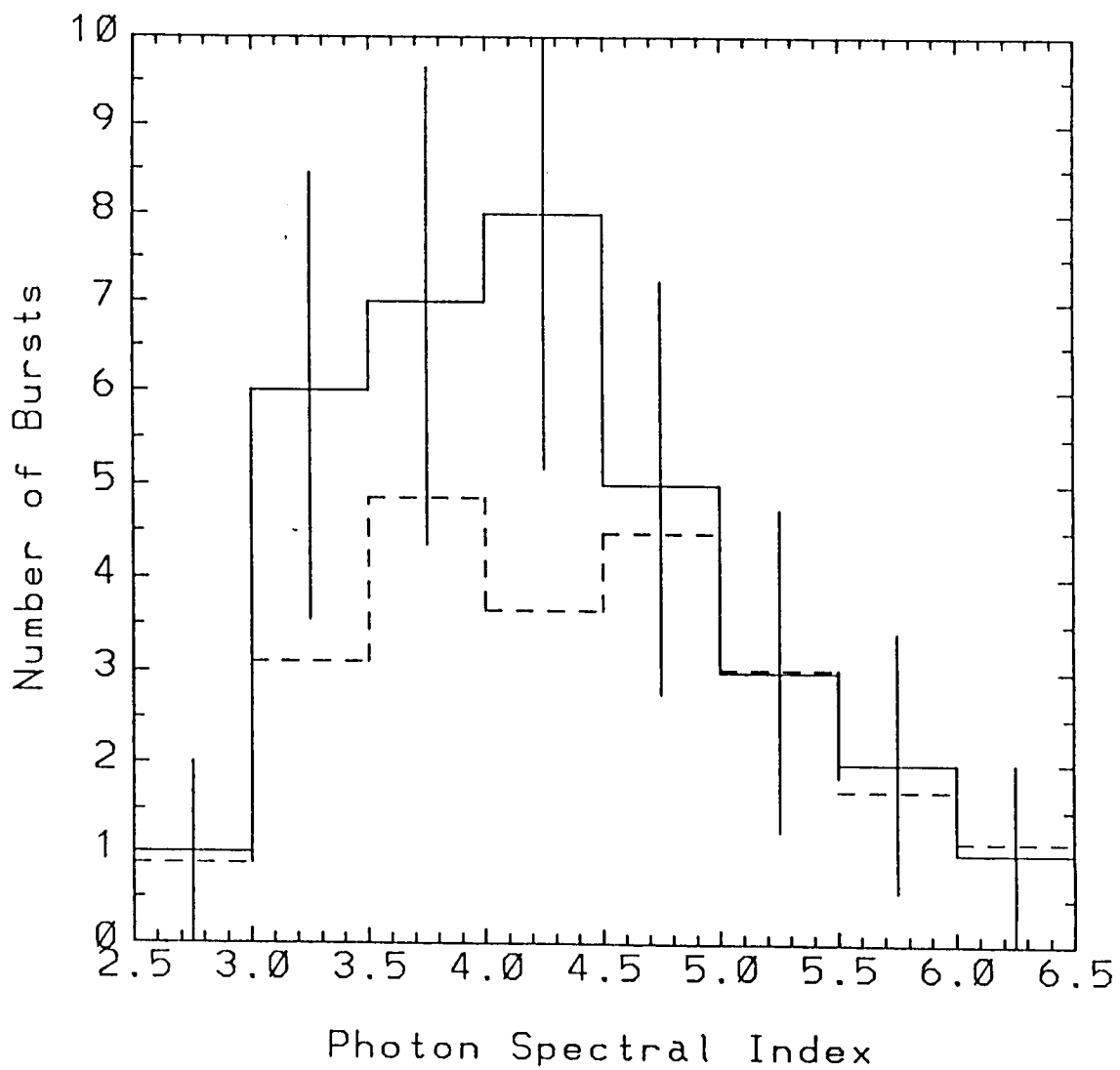


Fig. 9. The number of observed correlated bursts (solid) and the expected number of correlated bursts (dashed) as a function of X-ray spectral index.

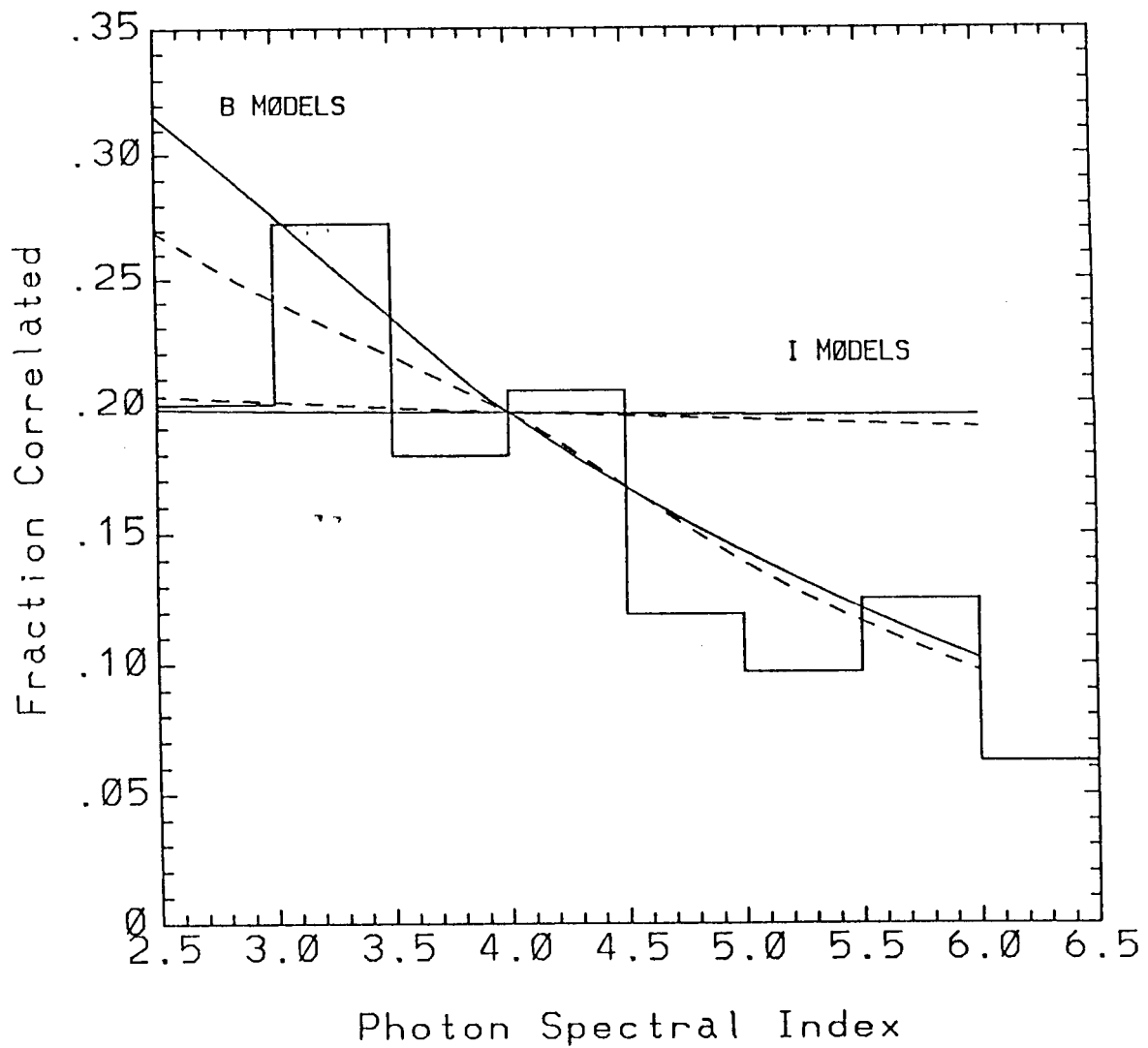


Fig. 10. The observed fraction of correlated events as a function of spectral index $f(\gamma)$ is shown (histogram) along with the predictions of the PL models of Table 3. Models B1 and I1 are shown as solid lines while B5 and I5 are dashed.